

Chiral Perturbation Theory tests at NA48 and NA62- R_K experiments at CERN

Flavio Costantini¹ for the NA48/2 Collaboration : Cambridge, CERN, Dubna, Chicago, Edinburgh, Ferrara, Firenze, Mainz, Northwestern, Perugia, Pisa, Saclay, Siegen, Torino, Wien and the NA62- R_K Collaboration: Birmingham, CERN, Dubna, Fairfax, Ferrara, Firenze, Frascati, Mainz, Merced, Moscow, Napoli, Perugia, Pisa, Protvino, Roma I, Roma II, Saclay, San Luis Potosi, Stanford, Sofia, Torino, TRIUMF.

¹Dipartimento di Fisica, Università di Pisa and INFN Pisa
Largo B. Pontecorvo 3, 56127 Pisa (Italy)

DOI: <http://dx.doi.org/10.3204/DESY-PROC-2014-04/16>

Final results from an analysis of about 400 $K^\pm \rightarrow \pi^\pm \gamma \gamma$ rare decay candidates collected by the NA48/2 and NA62- R_K experiments at CERN during low intensity runs with minimum bias trigger configurations are presented. The results include a model-independent decay rate measurement and fits to Chiral Perturbation Theory (ChPT) description. The data support the ChPT prediction for a cusp in the di-photon invariant mass spectrum at the two pion threshold.

1 Introduction

The NA48/2 experiment at the CERN SPS has collected a large sample of charged kaon decays in 2003–04 (corresponding to about 2×10^{11} K^\pm decays in the vacuum decay volume). The experiment featured simultaneous K^+ and K^- beams and was optimized for the search for direct CP violating charge asymmetries in the $K^\pm \rightarrow 3\pi$ decays [1]. Its successor, the NA62- R_K experiment, collected a 10 times smaller K^\pm decay sample with low intensity beams and minimum bias trigger conditions in 2007–08. NA62- R_K used the same detector as NA48/2, while the data taking conditions were optimized for a measurement of the ratio of the rates of the $K^\pm \rightarrow \ell^\pm \nu$ decays ($\ell = e, \mu$) [2]. In particular, the main trigger chain required the presence of an electron (e^\pm).

The large data samples accumulated by both experiments have allowed precision studies of a range of rare K^\pm decay modes. Recent measurements of the rare decay $K^\pm \rightarrow \pi^\pm \gamma \gamma$ (denoted $K_{\pi\gamma\gamma}$ below) from the above data samples [3, 4] are reported here.

2 Beam and detector

The beam line has been designed to deliver simultaneous narrow momentum band K^+ and K^- beams derived from the primary 400 GeV/c protons extracted from the CERN SPS. Secondary beams with central momenta of 60 GeV/c (for NA48/2) or 74 GeV/c (for NA62- R_K) were used.

The beam kaons decayed in a fiducial decay volume contained in a 114 m long cylindrical vacuum tank. The momenta of charged decay products were measured in a magnetic spectrometer, housed in a tank filled with helium placed after the decay volume. The spectrometer comprised four drift chambers (DCHs), two upstream and two downstream of a dipole magnet which provided a horizontal transverse momentum kick of 120 MeV/c (for NA48/2) or 265 MeV/c (for NA62- R_K) to charged particles. Each DCH was composed of eight planes of sense wires. A plastic scintillator hodoscope (HOD) producing fast trigger signals and providing precise time measurements of charged particles was placed after the spectrometer. Further downstream was a liquid krypton electromagnetic calorimeter (LKr), an almost homogeneous ionization chamber with an active volume of 7 m³ of liquid krypton, 27 X_0 deep, segmented transversally into 13248 projective $\sim 2 \times 2$ cm² cells and with no longitudinal segmentation. The LKr information is used for photon measurements and charged particle identification. An iron/scintillator hadronic calorimeter and muon detectors, not used in the present analysis, were located further downstream. A detailed description of the detector can be found in Ref. [5].

3 The $K^\pm \rightarrow \pi^\pm \gamma\gamma$ decay in the ChPT

Measurements of radiative non-leptonic kaon decays provide crucial tests of Chiral Perturbation Theory (ChPT) describing weak low energy processes. The $K_{\pi\gamma\gamma}$ decay has attracted the attention of theorists over the last 40 years [6, 7, 8, 9], but remains among the least experimentally studied kaon decays.

In the ChPT framework, the $K_{\pi\gamma\gamma}$ decay receives two non-interfering contributions at lowest non-trivial order $\mathcal{O}(p^4)$: the pion and kaon loop amplitudes which depend on an a priori unknown $\mathcal{O}(1)$ parameter \hat{c} , and the pole amplitude. Higher order unitarity corrections from $K \rightarrow 3\pi$ decays modify the decay spectrum significantly; in particular, they lead to non-zero differential decay rate at zero di-photon invariant mass [8]. The total decay rate is predicted to be $\mathcal{B}(K_{\pi\gamma\gamma}) \sim 10^{-6}$, with the pole amplitude contributing 5% or less [8, 9]. The ChPT predictions for the differential rate $d\Gamma/dz$ with $z = (m_{\gamma\gamma}/m_K)^2$, where $m_{\gamma\gamma}$ is the di-photon invariant mass, for several values of \hat{c} , are presented in Fig. 1. These spectra exhibit a characteristic cusp structure at twice the pion mass due to the dominant pion loop amplitude.

Experimentally, the only published $K_{\pi\gamma\gamma}$ observation is that of 31 K^+ decay candidates in the kinematic region $100 \text{ MeV}/c < p_\pi^* < 180 \text{ MeV}/c$ (p_π^* is the π^+ momentum in the K^+ frame) by the BNL E787 experiment [10].

4 Measurements of the $K^\pm \rightarrow \pi^\pm \gamma\gamma$ decay

New measurements of the $K_{\pi\gamma\gamma}$ decay have been performed using two minimum bias data sets: 1) two special K^\pm decay samples collected by the NA48/2 experiment at $\sim 10\%$ of the nominal beam intensity during 12 hours in 2003 and 54 hours in 2004; 2) a subset of the NA62- R_K data sample collected over the whole duration of the data taking with downscaled trigger conditions with an effective downscaling factor of about 20. The employed trigger conditions required a time coincidence of signals in both HOD horizontal and vertical strip planes within the same quadrant and an energy deposit of at least 10 GeV in the LKr calorimeter. The resulting effective kaon fluxes used for the NA48/2 and NA62- R_K $K_{\pi\gamma\gamma}$ analyses are similar, but the background conditions and resolution on kinematic variables differ significantly. The $K_{\pi\gamma\gamma}$ decay rate was measured with respect to the normalization decay chain with a large and well

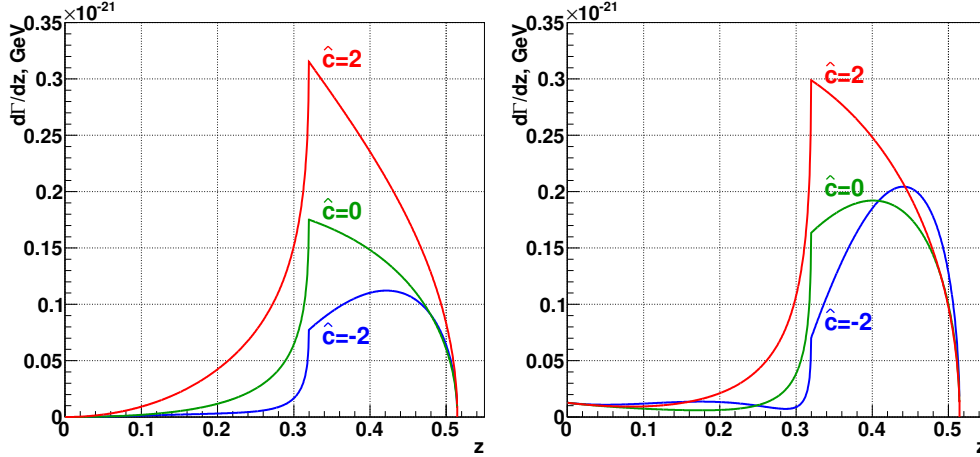


Figure 1: Differential rate ($d\Gamma/dz$) of the $K_{\pi\gamma\gamma}$ decays according to the $\mathcal{O}(p^4)$ (left) and $\mathcal{O}(p^6)$ (right) descriptions [7, 8] for several values of \hat{c} . The \hat{c} -independent pole contribution is also shown. For the $\mathcal{O}(p^6)$ parameterization, values of polynomial contributions [8] $\eta_i = 0$ and $K^\pm \rightarrow 3\pi^\pm$ amplitude parameters from a fit to experimental data [11] are used.

known branching fraction: the $K^\pm \rightarrow \pi^\pm \pi^0$ decay followed by the $\pi^0 \rightarrow \gamma\gamma$ decay. Signal and normalization samples have been collected with the same trigger logic.

Signal events are selected on the basis of spectrometer and LKr calorimeter information in the kinematic region $z = (m_{\gamma\gamma}/m_K)^2 > 0.2$ to reject the $K^\pm \rightarrow \pi^\pm \pi^0$ background, as well as other backgrounds from the π^0 decays, peaking at $z = (m_{\pi^0}/m_K)^2 = 0.075$. The residual background contamination is due to $K^\pm \rightarrow \pi^\pm \pi^0 \gamma$ and $K^\pm \rightarrow \pi^\pm \pi^0 \pi^0$ decays, with photons either missing the LKr acceptance or forming merged clusters in the LKr calorimeter. The event selection includes an upper limit for the transverse size of the LKr clusters, which reduces the background due to merged clusters. The $\pi^\pm \gamma\gamma$ invariant mass spectra of the selected $K_{\pi\gamma\gamma}$ candidates, with the expectations of the signal and background contributions from MC simulations, are displayed in Fig. 2: 149 (232) decay candidates with a background contamination of 10% (7%) are observed in the NA48/2 (NA62- R_K) data set.

A model-independent measurement of the z spectrum in the kinematic range $z > 0.2$ has been performed for the NA48/2 and NA62- R_K data sets. The partial branching fractions in bins of the z variable have been measured: they are model-independent because the considered z bin width is sufficiently small for the acceptances in z to have a negligible dependence on the assumed $K_{\pi\gamma\gamma}$ kinematical distribution. In addition, the y -dependence of the differential decay rate expected within the ChPT framework is weak [8, 9]. The final results of the measurements of the partial branching fractions in bins of the z variable are presented in Fig. 3 (left). The model-independent branching fraction in the kinematic region $z > 0.2$ is computed by summing over the z bins: $\mathcal{B}_{\text{MI}}(z > 0.2) = (0.965 \pm 0.061_{\text{stat}} \pm 0.014_{\text{syst}}) \times 10^{-6}$.

Measurements of the ChPT parameter \hat{c} have been made for both NA48/2 and NA62- R_K data samples by performing log-likelihood fits to the reconstructed z spectra. The data spectra of the z kinematic variable, together with signal and background expectations from simulations, are displayed in Fig. 3 (centre, right): they support the ChPT prediction of the cusp at $2m_\pi$ threshold. The values of the \hat{c} parameter in the framework of the ChPT $\mathcal{O}(p^4)$

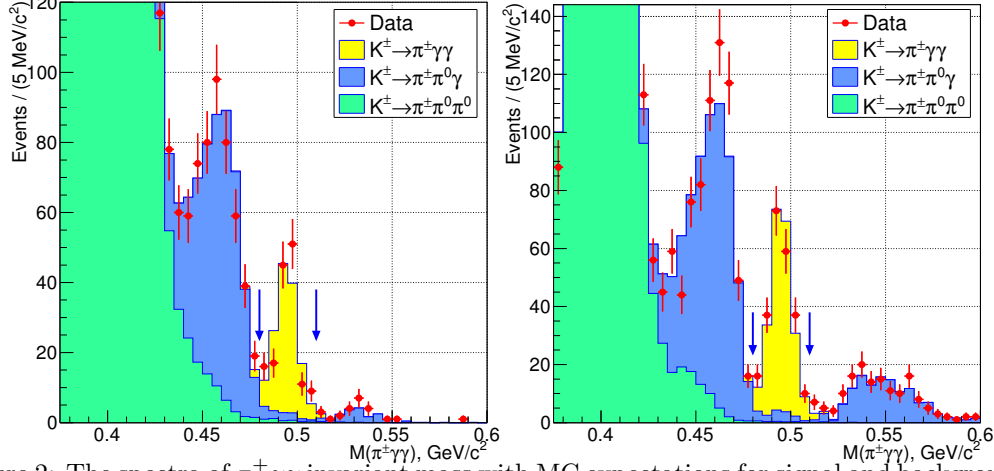


Figure 2: The spectra of $\pi^\pm\gamma\gamma$ invariant mass with MC expectations for signal and backgrounds: NA48/2 data (left) and NA62- R_K data (right). The signal region is between the 2 arrows.

$\mathcal{B}(K_{\pi\gamma\gamma}) \times 10^6$

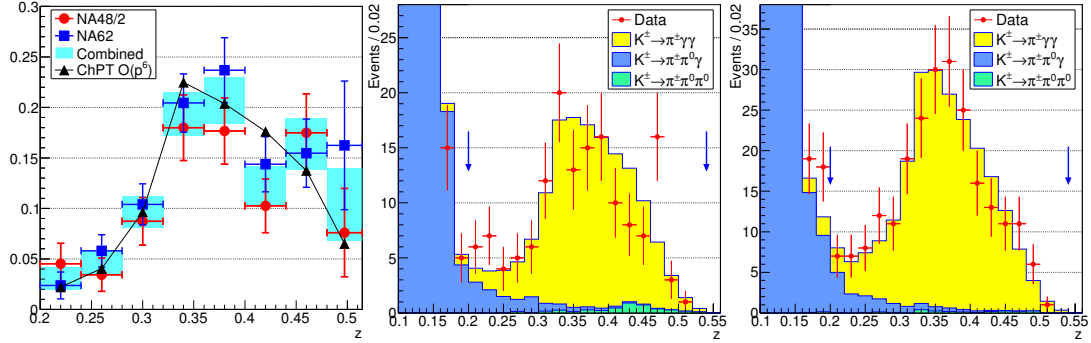


Figure 3: Left: measurements of partial model-independent branching fractions of the $K_{\pi\gamma\gamma}$ decay in bins of the z kinematic variable from the NA48/2 and NA62- R_K data samples. The spectra of $z = (m_{\gamma\gamma}/m_K)^2$ with MC expectations for signal (best fit) and backgrounds: NA48/2 data (centre) and NA62- R_K data (right). The signal region ($0.2 < z < 0.52$) is between the 2 arrows.

and $\mathcal{O}(p^6)$ parametrizations according to the formulation of [8] have been obtained. The $\mathcal{O}(p^6)$ parametrization involves a number of external inputs. In this analysis, they have been fixed as follows: the polynomial contribution terms are $\eta_1 = 2.06$, $\eta_2 = 0.24$ and $\eta_3 = -0.26$ as suggested in [8], while the $K^\pm \rightarrow 3\pi^\pm$ amplitude parameters come from a fit to the experimental data [11].

The results of the fits are presented in Table 1: they are in agreement with the earlier BNL E787 ones. A combination of results from the two experiments has been performed, taking into account the large positive correlation of the systematic uncertainties of the two measurements. The combined results are also presented in Table 1. The uncertainties are dominated by the statistical ones; the systematic errors on the combined results are dominated by those due to background subtraction. The branching ratio in the full kinematic range corresponding to the combined value of the \hat{c} parameter within the $\mathcal{O}(p^6)$ formulation is $\mathcal{B}(K_{\pi\gamma\gamma}) = (1.003 \pm 0.056) \times 10^{-6}$.

Table 1: Results of fits to the ChPT parameters [8] of the $K^\pm \rightarrow \pi^\pm \gamma\gamma$ di-photon mass spectra.

| | NA48/2 measurement | NA62- R_K measurement | Combined |
|------------------------------------|--|--|--|
| \hat{c} , $\mathcal{O}(p^4)$ fit | $1.37 \pm 0.33_{\text{stat}} \pm 0.14_{\text{syst}}$ | $1.93 \pm 0.26_{\text{stat}} \pm 0.08_{\text{syst}}$ | $1.72 \pm 0.20_{\text{stat}} \pm 0.06_{\text{syst}}$ |
| \hat{c} , $\mathcal{O}(p^6)$ fit | $1.41 \pm 0.38_{\text{stat}} \pm 0.11_{\text{syst}}$ | $2.10 \pm 0.28_{\text{stat}} \pm 0.18_{\text{syst}}$ | $1.86 \pm 0.23_{\text{stat}} \pm 0.11_{\text{syst}}$ |

References

- [1] J.R. Batley *et al.*, Eur. Phys. J **C52** (2007) 875.
- [2] C. Lazzeroni *et al.*, Phys. Lett. **B719** (2013) 326.
- [3] J.R. Batley *et al.*, Phys. Lett. **B730** (2014) 141.
- [4] C. Lazzeroni *et al.*, Phys. Lett. **B732** (2014) 65.
- [5] V. Fanti *et al.*, Nucl. Instrum. Methods **A574** (2007) 433.
- [6] L.M. Sehgal, Phys. Rev. **D6** (1972) 367.
- [7] G. Ecker, A. Pich and E. de Rafael, Nucl. Phys. **B303** (1988) 665.
- [8] G. D’Ambrosio and J. Portolés, Phys. Lett. **B386** (1996) 403.
- [9] J.-M. Gérard, C. Smith and S. Trine, Nucl. Phys. **B730** (2005) 1.
- [10] P. Kitching *et al.*, Phys. Rev. Lett. **79** (1997) 4079.
- [11] J. Bijnens, P. Dhone and F. Persson, Nucl. Phys. **B648** (2003) 317.